

A HIGH RESOLUTION SPECTROMETER FOR THE INVESTIGATION OF MOLECULAR STRUCTURES IN THE THZ RANGE

G.W. Schwaab
Physical Chemistry II, Ruhr-Universität Bochum
Universitätsstraße 150, Build. NC 7/71, D-44801 Germany

H.-W. Hübers, J. Schubert, Patrik Erichsen
DLR Institute of Space Sensor Technology
Rudower Chaussee 5, D-12489 Berlin

G. Gol'tsman, A. Semenov, A. Verevkin, S. Cherednichenko, E. Gershenson
MSPU, 1, M. Pirogowskaya St., 119435 Moscow, Russia

Abstract

A status report on the design study of a novel tunable far-infrared (TuFIR) spectrometer for the investigation of the structure of weakly bound molecular complexes is given. The goal is a sensitive TuFIR spectrometer with full frequency coverage from 1-6 THz. To hit the goal, advanced sources (e.g. p-Ge lasers) and detectors (e.g. superconducting hot electron bolometric (HEB) mixers) shall be employed to extend the technique of cavity ringdown spectroscopy, that is currently used at optical and infrared frequencies to the FIR spectral range. Critical for such a system are high-Q resonators that still allow good optical coupling, and wideband antireflection coatings to increase detector sensitivity and decrease optical path losses. 2nd order effective media theory and an iterative multilayer algorithm have been employed to design wideband antireflection coatings for dielectrics with large dielectric constants like Ge or Si. Taking into account 6 layers, for Si bandwidths of 100% of the center frequency could be obtained with power reflectivities below 1% for both polarizations simultaneously. Wideband dielectric mirrors including absorption losses were also studied yielding a bandwidth of about 50% with reflectivities larger than 99.5 %.

Introduction

Recent advances in terahertz (THz) technology allow the construction of improved tunable far-infrared (TuFIR) spectrometer systems, that can be used for the investigation of the structure of small molecular clusters. Ideally, such a system would cover several octaves (e.g. 0.5 to 6 THz) with a linewidth considerably below 1 MHz, and a sensitivity close to the quantum limit. If one wants to employ rapid detection or heterodyne detection, one needs a broad band low noise temperature mixer as detector and a widely tunable radiation source as local oscillator.

From the mixer side, superconducting hot electron bolometric (HEB) mixers have revolutionized heterodyne detection in the THz range, because they work as quantum detectors with low noise temperature and low local oscillator power needs ($< 1 \mu\text{W}$). Two possible realizations of the HEB differ according to the type of electron cooling mechanism used, either heat transfer to phonons via electron-phonon-interaction (phonon cooled HEB mixers)[1] or out-diffusion of hot electrons from the device (diffusion cooled HEB mixers)[2]. Recently, with a single phonon-cooled HEB mixer mounted in a spiral antenna on an elliptical Si lens low noise temperatures have been measured from 700 GHz to 5.2 THz[3]. Part of the optical losses (about 30% or 1.5 dB) are due to the reflection of the radiation at the Si-air surface.

From the local oscillator side several options are possible like BWOs (direct or multiplied), laser sideband generation[4,5,6], optical mixers[7,8], or p-type Ge lasers[9]. While laser sideband generation has been in use for more than a decade now, p-Ge lasers provide the most promising aspects for an improved spectrometer for the frequency range between 1 and 4 THz, since they are solid state devices with their maximum output power in the frequency range needed and they can be easily tuned by changing the magnetic field. The draw-backs of p-Ge lasers are their pulsed operation and their internal mode spacing which is defined by the length of the laser crystal. Improved systems should therefore be operated with an external resonator and anti-reflection coated front surfaces.

For spectroscopic applications, the pulsed laser still can be used. This has for example been done in the field of cavity ringdown spectroscopy[10], where instead of directly measuring the absorption of a gas, the Q-factor of a resonator cavity is measured with and without an absorbing gas. Briefly, a high-Q resonator is illuminated by a short laser pulse. At the resonator output an exponentially decaying series of signal pulses appears whose decay time is a measure of the resonator quality. An absorbing gas in the resonator will change this decay time in a way that the absorption coefficient can be calculated. The sensitivity of this method is extremely dependent on the reflectivity of the end mirrors. The higher the reflectivity, the more sensitive the spectrometer.

Summarizing, to be able to develop a new type of TuFIR spectrometer, two optical problems have to be tackled: first, the fabrication of wide-band anti-reflection coatings for the surfaces of Si lenses or the surface of a p-type Ge laser, and second, the design of wideband high-reflectivity FIR mirrors. To be able to theoretically study these problems, a computer program has been developed, that includes iterative handling of multilayer optical problems and second order effective media theory to simulate artificial dielectrics. In the following, the underlying theory of the code is described and some applications to wideband antireflection coatings and high-reflectivity FIR mirrors are shown.

Recursive Formalism for Multilayer Optics

The reflection and transmission of a multilayer optics can be calculated recursively by taking into account the reflections and transmissions at the boundaries between different layers and the phase delay within one layer. Figure 1 shows a N-layer system with layer thickness d_i , index of refraction n_i , and propagation angle θ_i for the i -th layer. With the incident electric field E_i , and the reflected electric field E_r , the total field reflection coefficient $\rho_j = \frac{E_r}{E_i}$ of layers $j+1$ through N is given by[11]

$$\rho_j = \frac{r_{j,j+1} + \rho_{j+1} e^{2i\delta_{j+1}}}{1 + r_{j,j+1} \rho_{j+1} e^{2i\delta_{j+1}}}$$

Here, $r_{j,j+1}$ represents the field reflection coefficient at the boundary of layers j and $j+1$, which is given by the Fresnel formulae[12], ρ_{j+1} the total field reflection coefficient of layers $j+2$ through N , i the $\sqrt{-1}$, and δ_{j+1} the phase delay in layer $j+1$. The phase delay is given by the relationship

$$\delta_j = 2\pi \frac{v}{c} n_j d_j \cos\vartheta_j$$

with c the velocity of light and θ_j the propagation angle of the radiation in layer j . The θ_j can be calculated from the incident angle θ_i using Snellius' law.

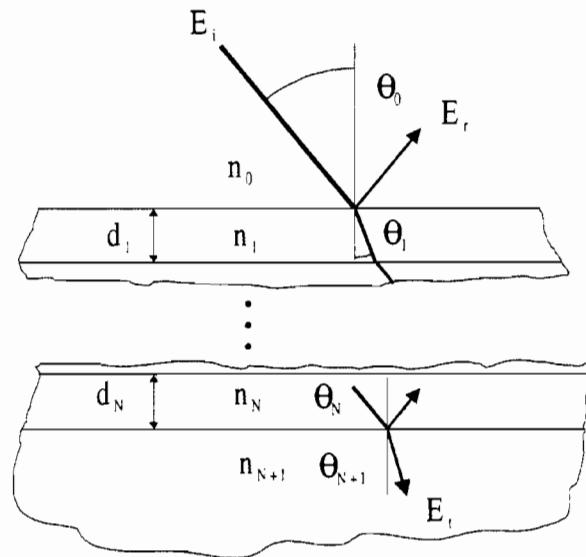


Figure 1: Schematic of a N-layer optics with incident field E_i , reflected field E_r , and transmitted field E_t . Each layer is described by its thickness d , its refractive index n , and its propagation angle θ .

For the total transmission τ_j of the multilayer optics, in a similar way the following formula can be derived:

$$\tau_j = \frac{\frac{n_{j+1} \cos \vartheta_{j+1}}{n_j \cos \vartheta_j} t_{j,j+1} \tau_{j+1} e^{i \delta_{j+1}}}{1 + r_{j,j+1} \rho_{j+1} e^{2i \delta_{j+1}}}$$

Here, $t_{j,j+1}$ represents the Fresnel field transmission factor at the boundary between layers j and $j+1$ as calculated by traversing from layer j into layer $j+1$. Please note, that for the transmission formula the layers are counted just opposite to the labeling in Figure 1 so that the numbers increase looking backward from the transmitted beam.

The power reflection and power transmission coefficients can be calculated from ρ_j and τ_j by taking the absolute square value, respectively. The phase shift is given by the overall argument of the expression. The formulae given here are based on plane-parallel surfaces and take not into account any walk-off effects due to Gaussian beam characteristics or a tilt between the different layers. However, they do include absorption effects: absorption can be characterized by a complex index of refraction, where the imaginary part represents the absorption in the medium. Both the Fresnel formulae and the Snellius law are still valid for complex indices of refraction (although, the angles θ_j become complex and more difficult to interpret).

2nd Order Effective Media Theory

Artificial dielectrics single layer antireflection coatings are well known in microwave technology and have been widely used for example to coat the surface of dielectric lenses[13]. Generally, they consist of a 1- or 2-dimensional periodic structure on the material surface, that is small enough to be seen as an effective dielectric medium by the incident wave. The advantage of artificial dielectric coatings is that they can be fabricated directly from the material in use and are therefore less susceptible to differential thermal expansion problems (e.g. for LHe systems). Also, in the frequency range between 1 and 6 THz there are not many materials available, that show low loss and good thermal behaviour as coatings for Si or other low-loss semiconductor optical elements.

The main disadvantage of such coatings at THz frequencies is their fabrication, since the dimensions necessary are between the dimensions manageable by mechanical means and those that can be etched. Only recently, new techniques, like laser ablation have been demonstrated, that can be used for fabricating those coatings.

The theory of one-dimensional antireflection structured surfaces is described in [11]. Incident radiation propagating in a dielectric with permittivity ϵ_i is partly transmitted through the surface of a dielectric with permittivity ϵ_t (see Figure 2). To minimize reflection losses, the surface is ruled with tapered grooves, that are approximated by a 1-dimensional step-function. The period of the grating is Λ , it's grating vector is K .

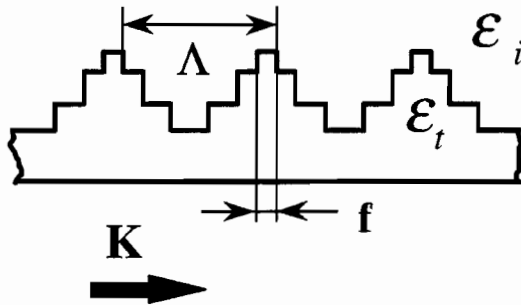


Figure 2: Multilayer antireflection coating between dielectrics with permittivities ϵ_i and ϵ_t by one-dimensional periodic surface grating. Λ is the grating period, K the grating vector, and f the filling factor of the grating.

The index of refraction at each level of the step function can be described by second order effective media theory. To be sure that no surface waves are generated by the grating, and that only the 0th diffraction order can be excited, one has to ensure that the design constant β fulfills the relationship

$$\beta = \frac{\lambda}{\Lambda} \frac{1}{n_i + n_t} \geq 1$$

with λ the wavelength of the wave, and n_i and n_t the indices of refraction of the incident and transmitting medium, respectively. For large values of β the grating period Λ becomes small which complicates fabrication of the

structure. On the other hand, if β becomes smaller than unity, at certain angles higher orders can be diffracted. Thus, β is typically chosen to be unity ($\beta=1$).

One-dimensional surface gratings create birefringence for the two polarizations with the field vector E perpendicular to K and E parallel to K . To second order theory, the relationships are:

$$\epsilon_{E \perp K}^{(2)} = [f \epsilon_t + (1-f) \epsilon_i] \left[1 + \frac{1}{\beta^2} \frac{\pi^2}{3} f^2 (1-f)^2 \frac{(\alpha_n - 1)^2}{1 + f(\alpha_n^2 - 1)} \right]$$

for E perpendicular to K with f the fraction of the grating period that is filled with permittivity ϵ_t , and $\alpha_n = n_t / n_i$. For E parallel to K , the expression is

$$\epsilon_{E \parallel K}^{(2)} = \left[\frac{f}{\epsilon_t} + \frac{(1-f)}{\epsilon_i} \right]^{-1} \left[1 + \frac{1}{\beta^2} \frac{\pi^2}{3} f^2 (1-f)^2 \frac{f(\alpha_n^2 - 1)}{\alpha_n^2 - f(\alpha_n^2 - 1)^2} \right]$$

Note, that in both formulae the expression in the left bracket gives the 0th order approximation as it can be found for example in [13].

Wideband Anti-Reflection Coatings for Highly Refractive Materials

To achieve the goal of wideband FIR antireflection coatings, second order effective media theory for one-dimensional surface gratings has been combined with the multilayer formula to optimize the index of refraction gradient.

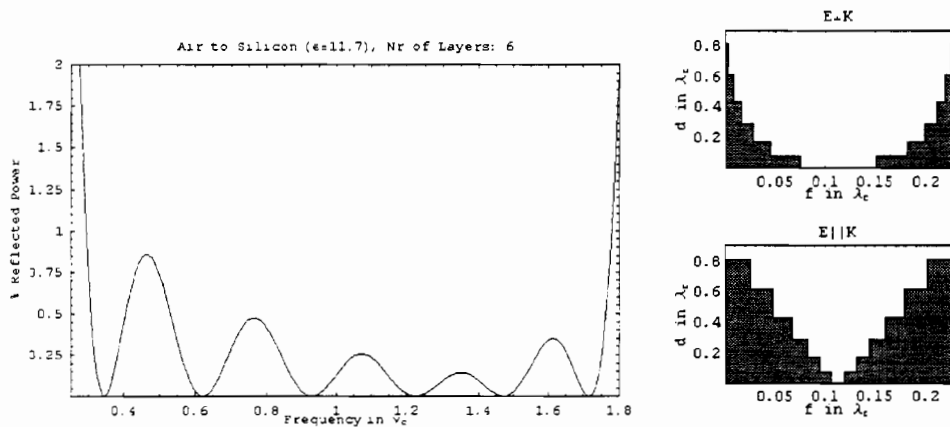


Figure 3: left: Power reflected off an air-silicon transition antireflection coated with a 6 layer one-dimensional surface grating. The coating has been optimized for single polarization radiation, the frequency is given relative to the design frequency ν_c . Right: the optimized shape of the grooves for the E-field perpendicular to the K-vector (above) and parallel to the K-vector (below). All dimensions are relative to the design wavelength λ_c .

In the mm-wave to FIR region most dielectrics change their index of refraction only slightly, if at all[13]. Therefore it is advantageous to calculate optimized grooves in a wavelength independent way; i.e. grating period, layer thickness, layer spacing, and

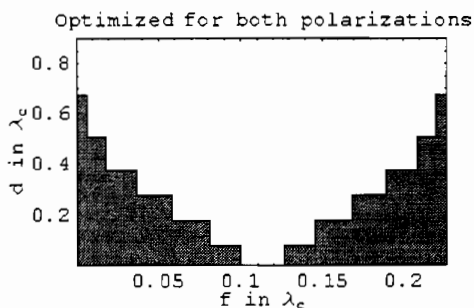


Figure 4: Groove shape optimized for minimum reflection for arbitrary polarization. Dimensions are given in units of the design wavelength

the bandwidth of the coating are given in relative frequencies for a particular index of refraction. The result may then be used to tailor the coating for the application frequency range.

Numerical optimization was used to minimize the power reflection for a given ratio ν_{\max}/ν_{\min} and to calculate optimized groove sizes. Figure 3 shows the bandwidth that can be achieved for singly polarized radiation for an air-Si ($\epsilon=11.7$) transition with a 6 layer antireflection coating. While the single surface

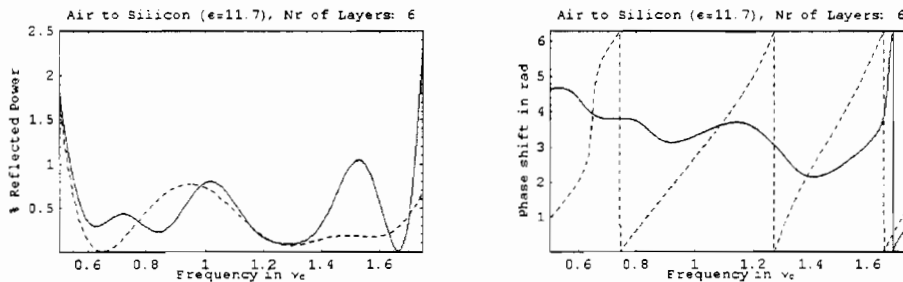


Figure 5: left: Power reflected off an air-silicon transition antireflection coated with the 6 layer one-dimensional surface grating shown for E perpendicular K (solid line) and E parallel K (dashed). The coating has been optimized for minimum reflection for both polarizations. Right: phase shift for both polarizations.

power reflection of an air-Si transition is 30%, a power reflection of less than 1 % can be achieved over $v_{\max}/v_{\min} \approx 6$. The birefringent behavior of the method is demonstrated by the different groove shapes necessary for the E-field of the incident light perpendicular and parallel to the K-vector of the grating, respectively, to achieve the same AR-performance.

The same number of AR-layers can also be optimized to achieve minimum reflection for both polarization directions simultaneously. The optimized groove shape is shown in Fig. 4. The total thickness of the AR coating is smaller than that for single polarization coatings, and the shape lies in between those for the two single polarization cases.

The reflected power as well as the phase shift versus frequency for both polarizations is shown in Figure 5. Again, the power reflection is below 1% for both polarizations. However, the bandwidth is reduced to $v_{\max}/v_{\min} \approx 3$. Although the reflectivities are about the same for both polarisations, the phase shift versus frequency behaves very different: for $E \perp K$ the phase shows only minor changes over most of the frequency band, while for $E \parallel K$ the phase is continuously increasing.

Wideband Dielectric Mirrors for High-Q THz Resonators

The multilayer algorithm has also been used to investigate high-reflectivity FIR mirrors as they have to be used in resonators for advanced TuFIR spectroscopy. The simplest possible way to build such a mirror is stacking alternating $\lambda/4$ -layers of materials with high and low index of refraction (see Fig. 6, left). Calculations were performed for four $\lambda/4$ -layers of Si separated by $\lambda/4$ -layers of air. Fig. 6, right shows 1-R of such a system, R being the power reflection coefficient. For lossless material, reflectivities higher than 99.9 percent can be achieved with a relative bandwidth of more than 20%. Introducing a loss tangent of 12×10^{-4} as it has been described in the literature [13] leads to a reduced reflectivity of 99.8% maximum and a bandwidth of about 50% for reflectivities higher than 99.5%.

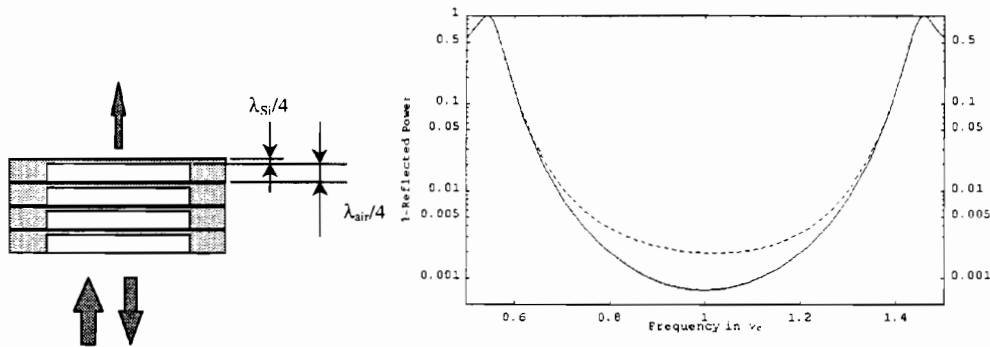


Figure 6: Left: Stack of four $\lambda/4$ doublets in air and Si as high-reflectivity FIR mirror. Right: 1-Reflectivity versus relative frequency for lossless Si (solid line) and Si with a loss tangent of 0.0012 (dashed).

Conclusions

Recursive multilayer optics in conjunction with 2nd order effective media theory can be used to design optimized wideband anti-reflection coatings for highly refractive dielectrics, and to design high-reflectivity mirrors for advanced TuFIR spectrometers. The AR coating will allow to get rid of the 30% optical losses in quasi-optical HEB mixers placed on Si lenses and also to minimize losses in pressure or cryostat windows in spectroscopic systems. For example, the pressure windows necessary for the HIFI instrument for FIRST could be built of quartz or Si with a 4 to 6 layer antireflection coating on both sides of the window. A single window could cover a frequency range from 450 to 1350 GHz with less than 2% loss at any particular frequency (scaling Fig. 5 with $\nu_c = 900$ GHz). The disadvantage of the coating, the different phase behavior of the polarization directions parallel and perpendicular to the K-vector of the grating can be overcome by using the same groove shape at perpendicular orientations at the front and back side of the window, respectively.

Similarly, taking into account newest results on wide-bandwidth HEB mixers [3], wideband THz receivers as they are currently being built for SOFIA can use the coatings to optimize receiver noise temperature from 1-3 THz or from 2-6 THz. The same holds for wideband sources, as for example optical mixers or p-type Ge lasers in external resonators.

The demonstration of the feasibility of high reflectivity FIR mirrors facilitates the design of new FIR resonators as they are needed for FIR cavity ringdown spectroscopy or for external resonators of p-type Ge lasers.

The next steps towards an advanced TuFIR spectrometer are the experimental verification of the theoretical investigations presented in this paper and their implementation into a spectroscopic system. Eventually, the extension of the frequency and power range accessible to TuFIR spectroscopy will lead to an

improved understanding of molecular systems as they can be found on earth and in space.

Acknowledgements: The Conference visit of G. Schwaab was supported by the Deutsche Forschungsgemeinschaft

References

- [1] E.M. Gershenzon, G.N. Goltsman, I. G. Gogidze, Yu.P. Gousev, A.I. Elantiev, B.S. Karasik, A.D. Semenov, *Sov. Phys. Superconductivity*, **3**(10), 1582, (1990)
- [2] D.E. Prober, *Appl.Phys.Lett.* **62**, 2119 (1993)
- [3] J. Schubert, A Semenov, G. Gol'tsman, H.-W. Hübers, G. Schwaab, B. Voronov, E. Gershenzon, „Noise Temperature and Sensitivity of a NbN Hot-Electron Mixer at Frequencies from 0.7 to 5.2 THz“, *Proceedings of the 10th International Symposium on Space Terahertz Technology, Charlottesville, Virginia, 1999.*
- [4] D.D. Bicanic, B.F.J. Zuidberg, A. Dymanus, *Appl. Phys. Lett.* **32**, 367 (1978) .
- [5] P. Verhoeve, E. Zwart, M. Drabbels, J.J. ter Meulen, W. L. Meerts, A. Dymanus, D. B. McLay, *Rev. Sci. Instrum.* **61**, 1612 (1990) .
- [6] G.A. Blake, K.B. Laughlin, R.C. Cohen, K.L. Busarow, D.H. Gwo, C.A. Schmuttenmaer, D.W. Steyert, R.J. Saykally, *Rev. Sci. Instrum.* **62**, 1701 (1991)
- [7] S. Matsuura, G.A. Blake, R.A. Wyss, J.C. Pearson, C. Kadow, A.W. Jackson, A.C. Gossard, *Traveling-Wave Photmixers Based on Noncollinear Optical/Terahertz Phase-Matching*, *Proceedings of the 10th International Symposium on Space Terahertz Technology, Charlottesville, Virginia, 1999.*
- [8] E. Duerr, K. McIntosh, S. Verghese, „Design of a Distributed Photomixer for Use as Terahertz Local Oscillator, . *Proceedings of the 10th International Symposium on Space Terahertz Technology, Charlottesville, Virginia, 1999*
- [9] E. Bründermann, D.R. Chamberlain, E.E. Haller, „Novel Design of Widely Tunable Germanium Terahertz Lasers“, to be published in *Infrared Physics and Technology*, 1999
- [10] J.J. Scherer, D. Voelkel, D.J. Rakestraw, J.B. Paul, C.P. Collier, R.J. Saykally, A.O. Keefe, *Chem. Phys. Lett* **245**, 273-280 (1995)
- [11] D.H. Raguin, G.M. Morris, *Appl. Optics* **32**, 1154 (1993)
- [12] Bergmann-Schaefer, *Lehrbuch der Experimentalphysik Band III, Optik*, 7th Edition, p. 452, Walter de Gruyter, Berlin 1978,
- [13] P.F. Goldsmith, „*Quasioptical Systems*“, Chapter 5.4, IEEE press, New York, 1998